AD_____

Award Number: W81XWH-04-1-0870

TITLE: Optical Strategies for Studying Metastatic Mechanisms, Tumor Cell Detection and Treatment of Prostate Cancer.

PRINCIPAL INVESTIGATOR: Nicolas Solban, Ph.D.

CONTRACTING ORGANIZATION: Massachusetts General Hospital
Boston, MA 02114

REPORT DATE: October 2005

TYPE OF REPORT: Annual Summary

PREPARED FOR: U.S. Army Medical Research and Materiel Command
Fort Detrick, Maryland 21702-5012

REPORT DOCUMENTATION PAGE

Form Approved
OMB No. 0704-0188

1. REPORT DATE	2. REPORT TYPE	3. DATES COVERED
01-10-2005	Annual Summary	15 Sep 2004 – 14 Sep 2005

4. TITLE AND SUBTITLE
Optical Strategies for Studying Metastatic Mechanisms, Tumor Cell Detection and Treatment of Prostate Cancer.

5a. CONTRACT NUMBER

5b. GRANT NUMBER
W81XWH-04-1-0870

5c. PROGRAM ELEMENT NUMBER

6. AUTHOR(S)
Nicolas Solban, Ph.D.

5d. PROJECT NUMBER

5e. TASK NUMBER

5f. WORK UNIT NUMBER

7. PERFORMING ORGANIZATION NAME(S) AND ADDRESS(ES)
Massachusetts General Hospital
Boston, MA 02114

8. PERFORMING ORGANIZATION REPORT NUMBER

9. SPONSORING / MONITORING AGENCY NAME(S) AND ADDRESS(ES)
U.S. Army Medical Research and Materiel Command
Fort Detrick, Maryland 21702-5012

10. SPONSOR/MONITOR'S ACRONYM(S)

11. SPONSOR/MONITOR'S REPORT NUMBER(S)

12. DISTRIBUTION / AVAILABILITY STATEMENT
Approved for Public Release; Distribution Unlimited

13. SUPPLEMENTARY NOTES

14. ABSTRACT

Prostate cancer is the most common cancer in men. Current treatments have limitations due to undesirable side effects. The objective of this proposal is to evaluate the effect of photodynamic therapy (PDT) on prostate tumors in order to design optimal treatment regimens. We have established subcurative PDT conditions in 2 prostate cancer cell lines. Using these conditions we observed a transient decrease in adhesion to collagen IV, an abundant extracellular matrix protein, this correlated with a decrease in Integrin protein levels. We have also measured an increase in VEGF-A synthesis and release at these doses. We have established stably transfected GFP prostate cell lines and used a PSMA Ab to detect circulating prostate cancer cells. The results obtained establishes that PDT alters cellular-molecular processes such as cell adhesion, as well as transcription and synthesis of VEGF-A in vivo and in vitro at subcurative doses. We conclude that the most effective application of PDT for long-term cure, may involve combined therapeutic regimens.

15. SUBJECT TERMS
Cancer, Optical Imaging, Prostate, Metastasis, Treatment, Photodynamic Therapy, Biological Response.

16. SECURITY CLASSIFICATION OF:			17. LIMITATION OF ABSTRACT	18. NUMBER OF PAGES	19a. NAME OF RESPONSIBLE PERSON
a. REPORT	b. ABSTRACT	c. THIS PAGE			USAMRMC
U	U	U	UU	20	19b. TELEPHONE NUMBER *(include area code)*

Table of Contents

Introduction

Prostate cancer is the most commonly diagnosed cancer, and associated mortality is only second to lung cancer. Current treatments for localized prostate cancer include: surgery (radical prostatectomy), androgen suppression hormone therapy, radiation therapy, cryotherapy, chemotherapy, and watchful waiting. Although current treatment modalities are only palliative for metastatic prostate cancer, they provide potential curative treatments for organ-confined prostate cancer. However, these treatments have limitations since significant complications, such as urinary incontinence, impotence, and rectal complications can arise due to the damage of the surrounding tissue. Therefore, any new treatment that can destroy prostate cancer cells without risking injury to the surrounding tissue would be highly desirable for localized prostate cancer. Photodynamic therapy (PDT) represents a promising alternative for the treatment of recurrent prostate cancer.

Numerous preclinical studies demonstrated the feasibility of using PDT for the treatment of prostate cancer. The transport of PS in the canine prostate[1, 2] or in the rat prostate[3] as been investigated optically while the irradiation of canine prostate showed significant necrosis with minimal damage to the surrounding tissues[4, 5] with careful dosimetry. Two small clinical trials confirmed the effectiveness and low incidence of complications associated with PDT treatment of human prostate cancer. Both studies reported minimal damage to surrounding tissue and the preservation of the anatomical feature of the prostate. In the first trial Windahl et al.[6] treated 2 patients with localized tumors following prostate resection and found that PDT significantly reduced levels of the Prostate Specific Antigen (PSA) and did not cause any complications. In the second trial, Nathan et al.[7] reported cancer necrosis and decrease PSA levels in recurrent prostate cancer following radiation therapy. Furthermore, this was associated with a lower incidence of complications.

The objective of this proposal was to evaluate the effect of PDT on prostate tumors in order to design optimal treatment regimens. The primary hypothesis of this study is that PDT affects adhesion of prostate cancer cells to extracellular matrix proteins and induces Vascular Endothelial Growth Factor (VEGF) release. It is well established that VEGF can induce new vessel formation and vascular permeability. Together these events could lead to distant metastasis. We have also developed tools to detect circulating prostate cancer cells in live animals.

Body

The following section addresses the original statement of work by providing an up to date report of the progress.

Task 1: evaluation of the effect of PDT on prostate cancer cells (month 1-4).

a) In the current study we have used 2 prostate cancer cell lines. The LNCaP human prostate cancer cells initially isolated from a lymphnode biopsy are useful for studying early stage of prostate cancer since they are androgen-dependant and have low metastatic potential. We have also used the MatLyLu (MLL) rat prostate cancer cells. These cells are useful for studying late stage prostate cancer since they are androgen independent and highly metastatic. Cells were incubated with [140 nM] of the photosensitizer BPD for 1 h, and then irradiated with a 690 nm laser at different light doses. 24 h following treatment cell viability was assayed using the standard MTT assay (Figure 1). Since this proposal is interested in the effect of subcurative PDT we have chosen the following light doses for LNCaP: 0.25 J/cm^2 and 0.5 J/cm^2, which correspond to 85% and 65% survival respectively and 1 J/cm^2 and 3 J/cm^2 for MLL, which corresponds to 65% and 20% survival respectively.

b) We have used the conditions established in task 1(a) to test the adhesion of PDT treated MLL cells to the extracellular matrix protein collagen IV. MLL cells were treated with 140 nM BPD for 1 h and irradiated with 1 J/cm^2 and 3 J/cm^2. 24 h and 72 h following treatment cells were collected and plated on

collagen IV plates and left to adhere for 4 h. % adhesion of cells was calculated by dividing the number of cells after washing to the total number of cells plated. Following subcurative PDT, MLL cells have a decrease adhesion to collagen IV (**Figure 2**, left graph). At the higher light dose (3 J/cm^2) the adhesion is reduced to 15%. However this decrease is transient since after 72 h the adhesion is back to control level (**Figure 2**, right graph).

c) In order to determine which adhesion molecules are affected by subcurative PDT we have hybridized a rat extracellular matrix and adhesion molecule microarray with RNA extracted from MLL cells treated with 3 J/cm^2. This array contains 111 genes important for cell adhesion. Analysis revealed 33 genes decreased following PDT, while none were increased by treatment. Table 1 shows the genes that are more than 4 fold inhibited by treatment. The most inhibited gene is Integrin α5 with more than 7 fold inhibition. Interestingly, adhesion to collagen IV can be mediated by Integrin $\alpha5\beta1$[8], a heterodimeric protein composed of integrin α5 and integrin β1. Since we observed a decrease in adhesion to collagen IV (**Figure 2**) and a decrease in Integrin α5 (Table 1), we decided to measured Integrin β1 levels post PDT. Figure 3 shows a western analysis of Integrin β1 levels. Subcurative PDT causes a transient decrease in Integrin β1 levels 24 h after treatment (Figure 3, A), however 72 h post-PDT Integrin β1 levels are back to control levels (Figure 3, B).

To study the *in vivo* effect of PDT on cell adhesion we used an orthotopic model of prostate cancer generated with MLL cells. The prostate tumor develops rapidly; after 7 days a 0,5 cm^3 tumor is treated with subcurative PDT (50 J/cm^2), 24 h following treatment tumors were fixed in 10 % formalin and embedded in paraffin. Tissue slices were stained with a β1-integrin Ab. Immunohistochemical analysis reveals a decrease in β1-Integrin staining following PDT (Figure 4, compare right panels). Interestingly, in Figure 4 (bottom panels) we can see an area of the tumor that did not receive enough light or PS to destroy it. In that region β1-integrin levels are similar to control animals.

d) We have used an ELISA to specifically measure VEGF production after subcurative PDT treatment of LNCaP cells using the conditions established in task 1(a). **Figure 5** (A) shows the quantification of secreted VEGF from LNCaP cells, 24 h after subcurative PDT. We observe a significant increase in secreted VEGF at both doses used (1,6 and 2.0 fold increase). To study the mechanism of this release we collected cells 24 h post treatment and measured intracellular VEGF levels by ELISA, results were normalized to protein concentration. We observed a significant increase ($p<0.05$) in intracellular VEGF-A (**Figure 5**, B) at 0,5 J/cm^2 (1.6 fold). Surprisingly we did not measure any significant increase in intracellular VEGF-A levels at the lower dose (0,25 J/cm^2). VEGF-A is known to be regulated at the transcriptional and post-transcriptional levels. We therefore used primers specific for exon 1 and exon 8 of VEGF-A in order to determine the mechanism of VEGF-A increase post PDT. These primers can amplify all isoforms of VEGF-A. 3 isoforms were found to be expressed in LNCaP cells: VEGF121, VEGF144, and VEGF165 with VEGF121 being the most abundant and VEGF165 being the least. **Figure 5**,C shows the average fold induction of each VEGF-A isoform following GAPDH normalization. Concordant with intracellular protein levels there's a significant ($p<0,05$) increase in VEGF-A mRNA levels (1,6 fold) only after 0,5 J/cm^2 treatment, suggesting that PDT regulates VEGF-A at transcriptional levels only at the higher light dose.

To study the *in vivo* effect of subcurative PDT we have used an orthotopic prostate cancer model. This model is well established in our laboratory, therefore 3 weeks after LNCaP injection a 0,4 cm^3 tumor will develop in 90% of cases. *In vivo* PDT is performed 1 h after injection of LBPD. 690 nm light was delivered with a fluence rate of 100 mW/cm^2 and a total fluence of 50 J/cm^2, this treatment was shown to be subcurative, but still causes significant tumor damage. Therefore, it is ideal to study the response of tumors that have been exposed to both PS and light but not enough to kill them. 24 h following treatment tumors were fixed in 10 % formalin and embedded in paraffin. Tissue slices were stained with a VEGF-A Ab. Immunohistochemical analysis shows a more intense VEGF-A staining in

PDT treated tumors (**Figure 6** bottom pictures, compare PDT to NT and to BO). **Figure 6** top pictures show the hematoxylin and eosin staining of tumor sections. Notice numerous area of cell death observed after PDT treatment (**Figure 6**, arrows) indicative of effective treatment. To have a more quantitative approximation of the VEGF-A increase we collected proteins from tumors 24 h after treatments and a VEGF-A ELISA was performed, all results are normalized to protein concentration. Confirming our initial observation there is a significant ($p<0,03$) 2 fold increase in VEGF-A levels following PDT treatment (**Figure 7**) of orthotopic prostate tumors.

Task 2: Design of optical monitoring tools to detect circulating prostate cancer cells.
a) Since the Prostate Specific Membrane Antigen (PSMA) is expressed almost exclusively on prostate cancer cells it is a reliable marker for the detection of circulating prostate cancer cells. We have tested the expression of PSMA in LNCaP and MLL cells by western analysis. Figure 8 shows that PSMA is expressed only in LNCaP cells both *in vitro* and *in vivo*. Furthermore PDT treatment of LNCaP tumors does not affect PSMA expression. On the other hand PSMA is not expressed in MLL cells *in vitro* or *in vivo*. Therefore PSMA cannot be used to detect circulating MLL cells. Other methods for detecting these cells are currently under investigation.

b) We have labeled PSMA Ab with the fluorescent dye Cy5.5, or Cy5. The free dye was separated from conjugated antibody using a gel filtration column. Using this conjugation method we obtained a dye/antibody ratio of about 3 and a recovery of about 90%. To confirm that labeled PSMA maintained its specificity we have incubated LNCaP cells and MLL cells with 5 μg of labeled PSMA for 15 min at 37°C. Similar to western blot results, Figure 9 shows that only LNCaP cells are labeled by PSMA, confirming that PSMA-Cy5.5 maintained its specificity.

c) LNCaP cells were labeled with PSMA-Cy5.5, PSMA- Cy5, or with PSMA-Qdots. Fluorescence was measured by FACS. As shown in Figure 11, LNCaP cells labeled with PSMA-Qdots are about 10x brighter than LNCaP cells labeled with PSMA-Cy5. We were not able to detect LNCaP cells labeled with PSMA-Cy5.5 since the instrument doesn't have the proper filters. These cells were then injected in the tail vain of SCID mice and the animals were placed on the *in vivo* cytometer to detect circulating cells. We were not able to detect cells labeled with PSMA-Cy5 or cells labeled with PSMA-Cy5.5. However we were able to count cells labeled with PSMA-Qdots. Therefore for task 3 we will use PSMA-Qdots to detect circulating prostate cancer cells.

d) LNCaP and MLL cells were transfected with the plasmid pEGFP-N1 (Clontech). This plasmid codes for the green fluorescent protein (GFP). Stable cells were established after selection in the antibiotic G418. Highly fluorescent cells were sorted by FACS (Figure 10).

e) Stably tranfected GFP cells were injected in the tail vein of animals and the *in vivo* cytometer was used to detect them. However, we were not able to detect these cells even though they are very fluorescent (Figure 10). This is most likely due to the absorption of green fluorescence by blood. In order to detect circulating cancer cells we will use antibodies labeled with Qdots since we have shown in task II (c) that labeled cells are highly fluorescent and can easily be detected using the *in vivo* flow cytometer.

Task 3: Evaluation of cells shedding following PDT treatment.
In our initial statement of worked we had planned on starting this task in month 8. However due to the problems encountered with the detection of circulating cells we are slightly delayed. We will now use antibodies labeled with Qdots to perform this task, we still estimate completion of this task, as planned, by month 18.

Key Research Accomplishments

Travel Award:

- 2005, European Society for Photobiology: Postdoctoral Fellow Travel Award.
- 2004, American Society for Photobiology: Postdoctoral Fellow Travel Award.

Full proceedings of meeting:

- **Nicolas Solban**, Nathaniel Sznycer-Taub, Juan Manuel Benavides, Sung Chang, Irene Georgakoudi, Tayyaba Hasan. The need for optical imaging in the understanding and optimization of photodynamic therapy. In: Darryl J. Bornhop, Samuel I. Achilefu, Ramesh Raghavachari, Alexander P. Savitsky; Editors. Genetically Engineered and Optical Probes for Biomedical Applications III. Proc. SPIE Vol: 5704, p. 1-9.

Book Chapter:

- **Solban N**, Ortel B, Pogue B, Hasan, T. Targeted Optical Imaging and Photodynamic Therapy. In: A.A. Jr. Bogdanov and K Licha, editors. Molecular Imaging: An Essential Tool in Preclinical Research, Diagnostic Imaging, and Therapy. Heidelberg: Springer-Verlag, 2005: Chapter 12, 229-58

Abstract:

- Georgakoudi, **N. Solban**, C. Lin, T. Hasan. In vivo flow cytometry: A noninvasive method for monitoring circulating cells after PDT. *SPIE Optics East 2005*, Boston, MA, USA, 2005 (to be presented).
- **N Solban,** I Georgakoudi, W. Rice, C Lin, T Hasan. Decrease in adhesion of prostate cancer cells following subcurative photodynamic therapy. *11th Congress of the European Society for Photobiology*. Aix-les-Bains, France, 2005.
- **N Solban**, A Sinha, S Chang, W Rice, P K Selbo, T Hasan. Effect of photodynamic therapy on human prostate tumor microcirculation: potential mechanism of distant metastasis. *96th Annual meeting of the American Association for Cancer Research*, Anaheim, CA, USA, 2005

Conclusions

We have established subcurative PDT conditions in 2 prostate cancer cell lines. Using these conditions we observed a transient decrease in adhesion to collagen IV, an abundant extracellular matrix protein, this correlated with a decrease in Integrin protein levels. We have also measured an increase in VEGF-A synthesis and release at these doses. We have established stably transfected GFP prostate cell lines and used a PSMA Ab to detect circulating prostate cancer cells. The results obtained establishes that PDT alters cellular-molecular processes such as cell adhesion, as well as transcription and synthesis of VEGF-A in vivo and in vitro at subcurative doses. We conclude that the most effective application of PDT for long-term cure, may involve combined therapeutic regimens.

References

1. Zhu TC, Hahn SM, Kapatkin AS, et al. In vivo optical properties of normal canine prostate at 732 nm using motexafin lutetium-mediated photodynamic therapy. *Photochem Photobiol.* 2003;77:81-88.

2. Solonenko M, Cheung R, Busch TM, et al. In vivo reflectance measurement of optical properties, blood oxygenation and motexafin lutetium uptake in canine large bowels, kidneys and prostates. *Phys Med Biol.* 2002;47:857-873.

3. Hamblin MR, Rajadhyaksha M, Momma T, Soukos NS, Hasan T. In vivo fluorescence imaging of the transport of charged chlorin e6 conjugates in a rat orthotopic prostate tumour. *Br J Cancer.* 1999;81:261-8.

4. Chen Q, Huang Z, Luck D, et al. Preclinical studies in normal canine prostate of a novel palladium-bacteriopheophorbide (WST09) photosensitizer for photodynamic therapy of prostate cancers. *Photochem Photobiol.* 2002;76:438-445.

5. Hsi RA, Kapatkin A, Strandberg J, et al. Photodynamic therapy in the canine prostate using motexafin lutetium. *Clin Cancer Res.* 2001;7:651-660.

6. Windahl T, Andersson SO, Lofgren L. Photodynamic therapy of localised prostatic cancer. *Lancet.* 1990;336:1139.

7. Nathan TR, Whitelaw DE, Chang SC, et al. Photodynamic therapy for prostate cancer recurrence after radiotherapy: A phase I study. *J Urol.* 2002;168:1427-1432.

8. Runnels JM, Chen N, Ortel B, Kato D, Hasan T. BPD-MA-mediated photosensitization in vitro and in vivo: Cellular adhesion and beta1 integrin expression in ovarian cancer cells. *Br J Cancer.* 1999;80:946-953.

APPENDICES

Table 1: Genes inhibited by PDT.

Genebank	Gene Name	Description	Fold Inhibition
XM_235707	Itga5	Integrin α5	7.45
NM_012939	Ctsh	Cathepsin H	6.22
NM_133514	Mmp10	Matrix metalloproteinase 10	6.15
NM_053963	Mmp12	Matrix metalloproteinase 12	5.79
NM_020071	Fgb	Fibrinogen, β polypeptide	5.09
NM_031755	Ceacam1	Carcinoembryonic antigen-related cell adhesion molecule 1	4.91
XM_235796	MMP20	Similar to matrix metalloproteinase-20	4.51
XM_340884	ITGA3	Similar to VLA-3 α-subunit (LOC360606), mRNA	4.48
XM_222317	Mmp19	Similar to matrix metalloproteinase 19 (LOC304608), mRNA	4.28

Figure 1: Prostate cancer cell lines killing curve. LNCaP cells (left) or MLL cells (right) were incubated with BPD for 1 h and irradiated with different light doses. 24 h post-PDT viability was assayed. Grey bars show the light doses used in the subsequent experiments.

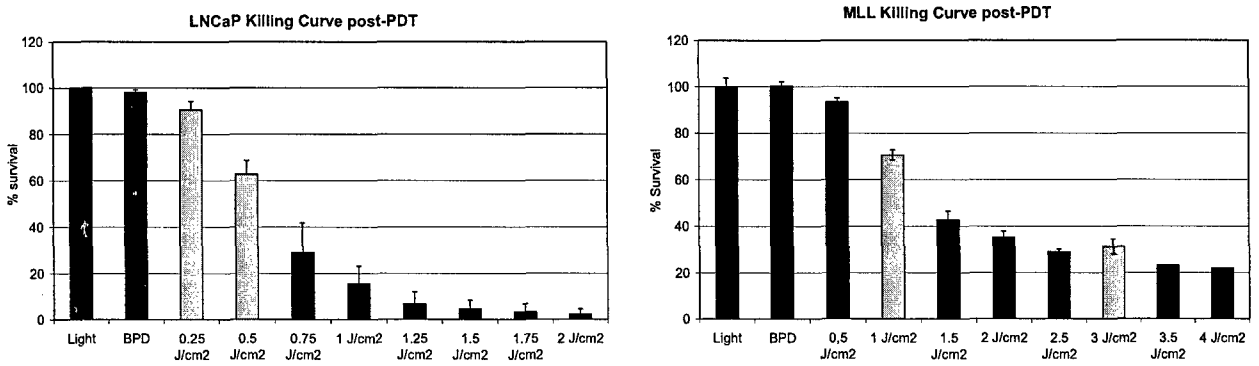

Figure 2: Transient decrease in adhesion following PDT. 24 h (left) and 72 h (right) after PDT MLL cells were collected and left to adhere for 4 h to collagen IV. % Adhesion was calculated by dividing the number of cells after washing to the total number of cells plated.

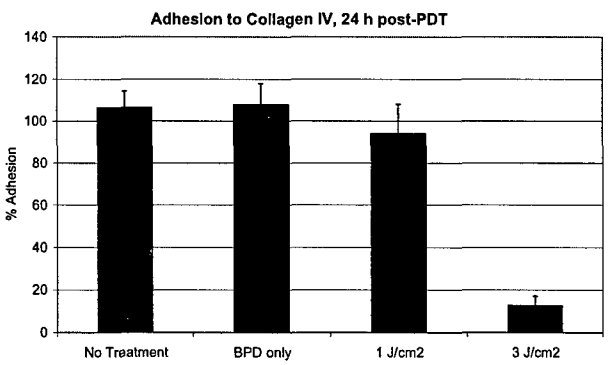

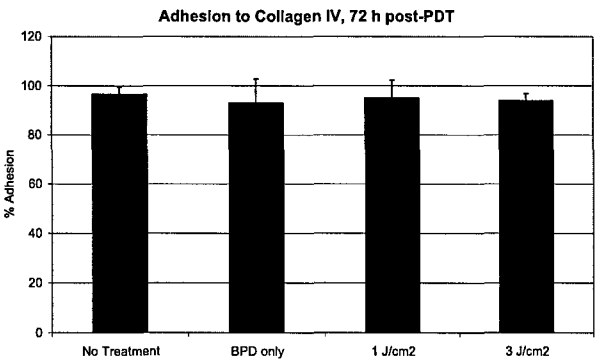

Figure 3: Decrease in Integrin β1 levels by subcurative PDT. 24 h following treatment (A) and 72 h following treatment (B) PDT treated cells were collected, protein was extracted and Integrin β1 western analysis was performed. There is a transient decrease in Integrin β1 levels after 24 h (A) but the levels return to normal 72 h after treatment (B). LO: light only, BO: BPD only. Actin was used as a loading control.

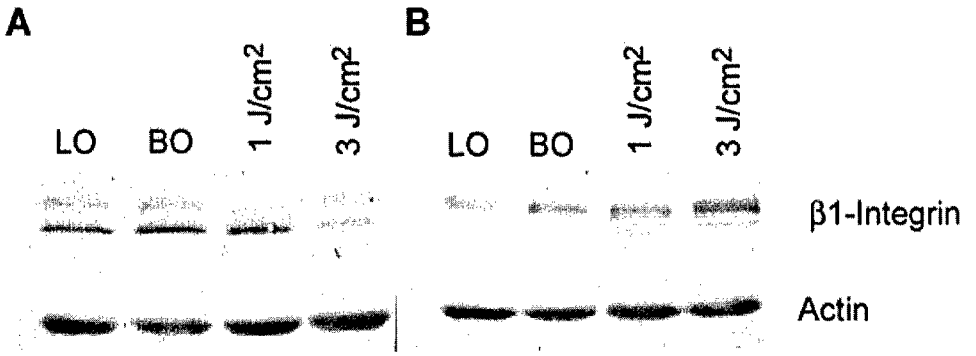

Figure 4: Imunohistochemical analysis for β1-Integrin. Orthotopic MatLyLu prostate tumors were PDT treated. 24 h post-treatment animals were sacrificed; the tumor was fixed in 10% formalin and embedded in paraffin. Immunohistochemistry using β1-Integrin Ab was performed on deparaffinized sections.

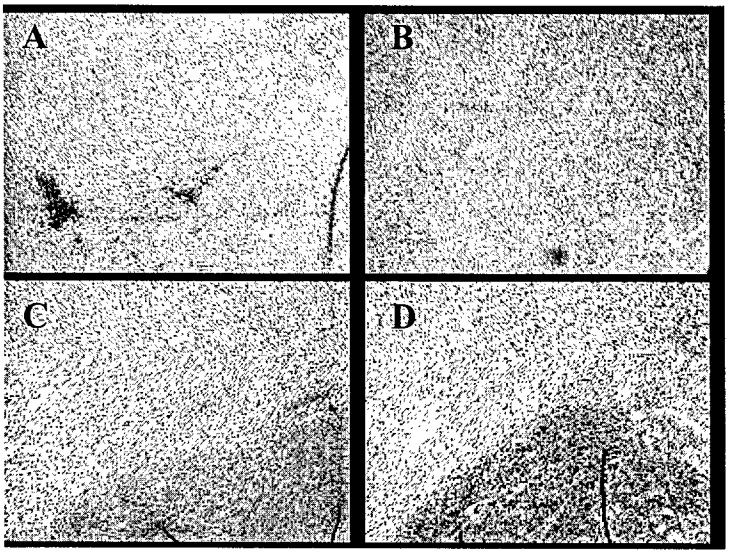

Figure 5: Subcurative PDT increases VEGF-A in vitro. Using a VEGF-A ELISA we have measured secreted VEGF (A), as well as intracellular VEGF levels (B). Secreted VEGF is increased at both subcurative doses used (A), while its intracellular levels are increased only in the higher PDT dose (B). We have performed RT-PCR analysis of VEGF-A mRNA using primers specific to exon 1 and to exon 8. This enable us to detect all VEGF isoforms expressed. Similar to intracellular levels, VEGF mRNA levels are only increased at the higher PDT dose (C). Values represent fold induction after calculating the ratio VEGF:GAPDH and arbitrarily setting NT as 1. Average values of 3 independent experiments measured in duplicate. (NT: no treatment, BO: BPD only, LO: light only).

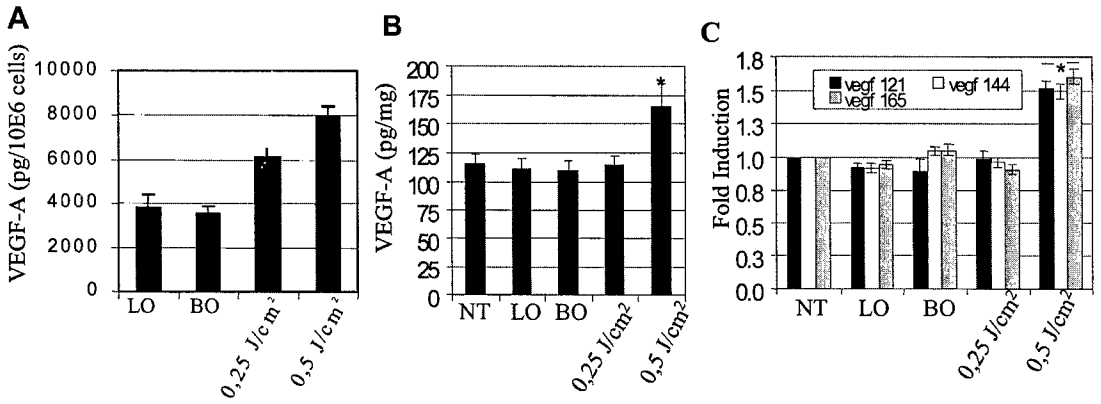

Figure 6: Immunohistochemical analysis for VEGF-A expression. 24 h following treatment animals were sacrificed and orthotopic prostate tumors were collected. Sections of paraffin-embedded tumors were stained using hematoxylin and eosin (H&E) method (top) or using VEGF mAb (bottom). NT: No treatment, BPD: drug only, PDT: treatment @ 50J/cm^2.

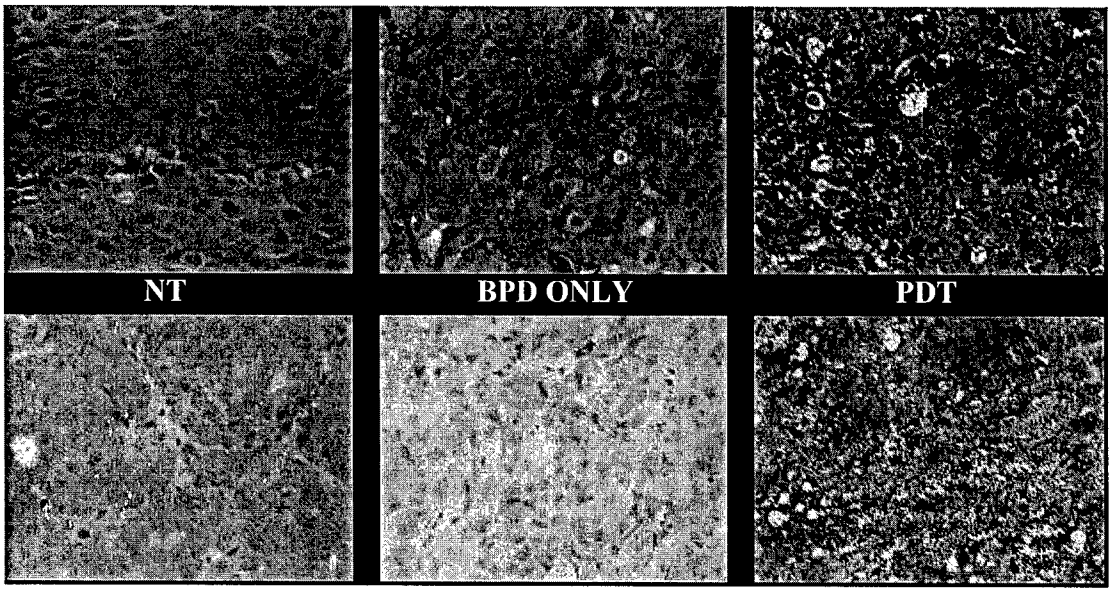

Figure 7: Subcurative PDT increases VEGF in vivo. Orthotopic LNCaP prostate tumors implanted in SCID mice were treated. 24 h post-treatment prostate tumors were collected, proteins were extracted and a VEGF ELISA was performed. There's a significant increase in VEGF following subcurative PDT.

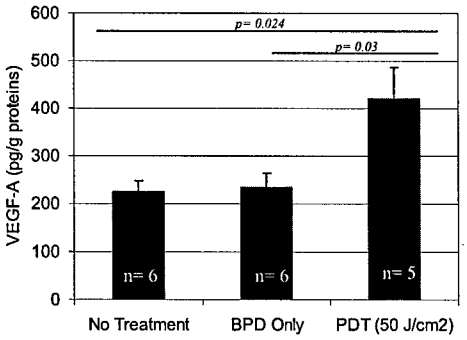

Figure 8: PSMA is expressed only in LNCaP cells. Western blot analysis shows expression of PSMA only in LNCaP cells both *in vitro* and *in vivo*. PDT treatment does not modify PSMA expression. PSMA is not detected in MLL cells.

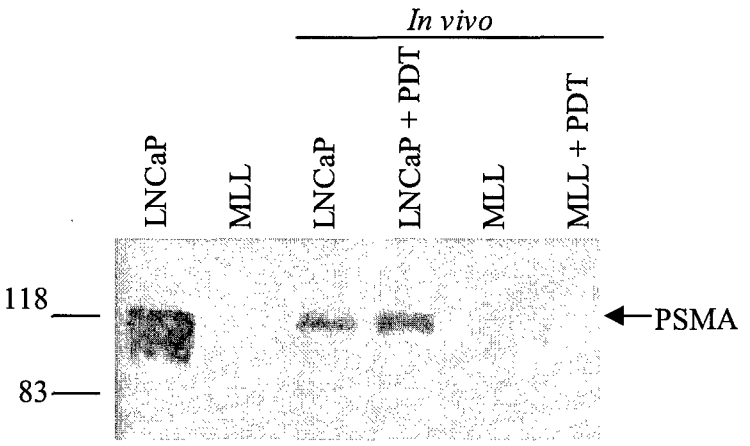

Figure 9: Specific labeling of LNCaP cells with PSMA-Cy5.5. LNCaP and MLL cells were incubated with 5 μg PSMA-Cy5.5 for 15 min at 37°C. After PBS washes cells were observed using a confocal microscope. LNCaP cells are specifically labeled while no labeling is observed in MLL cells.

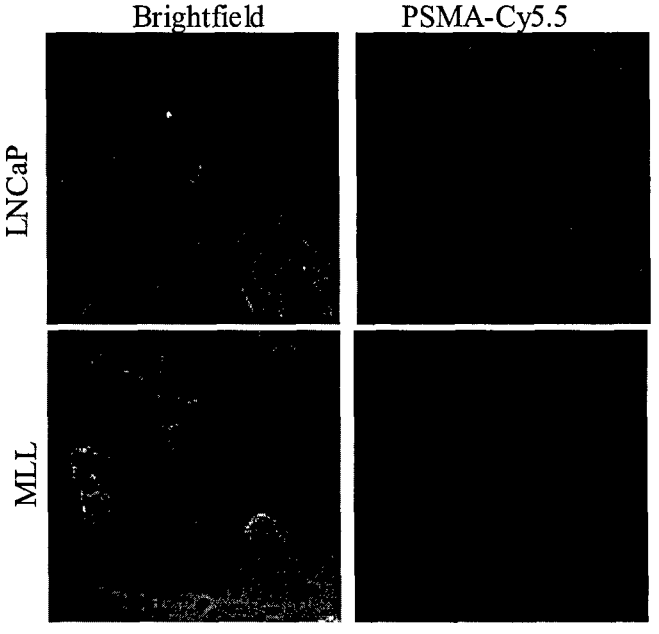

Figure 10: FACS analysis of GFP LNCaP and GFP MLL cells. Histogram of LNCaP-GFP and MLL-GFP before sorting. M1 represents cells with the highest fluorescence that were sorted. FL1-H is the channel used to detect green fluorescence.

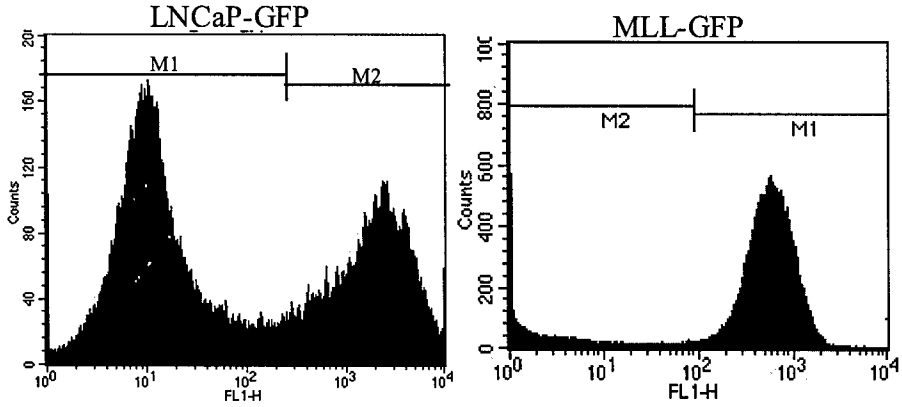

Figure 11: FACS Analysis of LNCaP cells. LNCaP cells were incubated with MLN, MLN-Cy5 or MLN-Qdots. MLN is a specific antibody to PSMA. Specific fluorescence is observed with Cy5 and Qdots.